# EXPERIMENTAL SHRINKAGE STUDY OF CERAMIC DLP 3D PRINTED PARTS AFTER FIRING GREEN BODIES IN A KILN

**IAROSLAV KOVALENKO, YUVARAJ RAMACHANDRAN, MARYNA GARAN**

Technical University of Liberec, Faculty of Mechanical Engineering, Department of Manufacturing Systems and Automation, Liberec, Czech Republic

**DOI : 10.17973/MMSJ.2019_03_2018113**

**e-mail:** iaroslav.kovalenko@tul.cz

The objective of this work was to investigate dimensional parameters of 3D printed parts from glass ceramic photopolymer before and after debinding and sintering in a kiln. During experiments batches of green bodies were printed with different layer thickness and curing strategy. We used 3D printer with ultraviolet LED as a light power source. The peak of intensity of the UV LED was in the range from 385 to 405 nm. DLP projector from Texas Instruments was used for mask projection. After printing, each batch of green bodies was cleaned and post-cured in a UV chamber. Then their dimensions were measured, overgrowth of each sample was calculated. The next stage of the experiment was kiln firing according to special firing schedule. Dimensions of final parts were measured again, and their shrinkage was calculated. The experiment proved high influence of printing parameters on the overgrowth of models and almost no influence on shrinkage of parts after firing.

**KEYWORDS**

3D printing, DLP, SLA, debinding, photopolymer.

## 1 INTRODUCTION

Development of Additive Manufacturing (AM) technologies started in the 1983 from the experiment of Chuck Hull in which he tried to solidify coating of a desk by UV laser which was very similar to laser used in classic laser printers [Wohlers 2016]. He observed that solid three-dimensional parts can be created layer by layer. This technology was later patented and named stereolithography (SL) [Hull 1986]. It used an UV laser which was placed above a vat with photopolymer. Laser beam was moving and solidified a photopolymer resin point by point [Wong 2012].

In subsequent years many different technologies were invented and patented. New generations of SL technology are well known by name Digital Light Processing (DLP) Stereolithography and LCD Stereolithography [Dudley 2003]. In both technologies a photopolymer resin solidifies by light of wavelength defined by properties of build material. The main difference of these technologies from classic stereolithography is that a full layer is solidified at one moment of the time by projecting a mask image of current layer. This principle is called Mask Projecting Stereolithography (MPSL). According to ISO/ASTM 52900 standard, all mentioned technologies belong to the category Vat polymerization.

In recent years, AM production of complex structures from ceramic materials was mostly provided by Fused Deposition Modeling (FDM), Selective Laser Sintering (SLS) and binder jetting technologies [Vail 1992; Yoo 1993; Agarwala 1995, 1996; Travitzky 2014; Franks 2017]. However recently the SL technologies have been used more and more in ceramic printing processes. They are represented by classic SL and MPSL technologies [Griffith 2005; Felzmann 2012; Mitteramskogler 2014; Travitzky 2014; Gmeiner 2015; Schwentenwein 2015; Li 2017; Lian 2017].

Photopolymerization of ceramic build materials is based on solidification of liquid suspension, which consist of ceramic parts suspended in the photopolymer solution, with UV light [Halloran 2011]. Then printed part called “green body” consists of ceramic particles that are bound together by solidified polymer that is called binder in this case. After printing, green body can be post-cured for polymer crosslinking. But this step depends on printing parameters and can be skipped. Mandatory part of ceramic printing process is debinding and sintering of green body in a kiln. During this process binding material disappears, green body shrinks, and final part is formed.

## 2 EXPERIMENTAL SETUP

Described experiment was provided on the prototype of desktop DLP printer. The printer was built at the Technical University of Liberec under the project aimed to support student’s research at the Department of Manufacturing Systems and Automation. Functional scheme of the printer is shown on the Fig. 1.

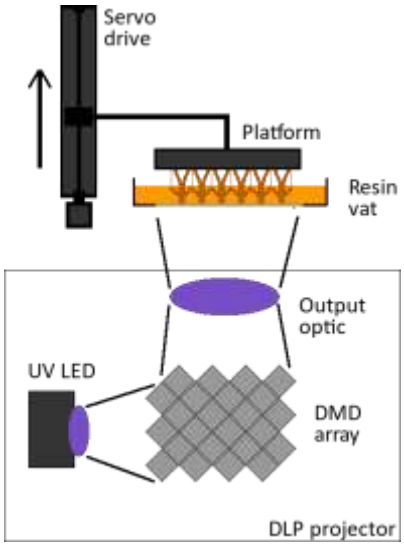


**Figure 1.** DLP printer functional scheme

### 2.1 *Description of the printer*

Basic idea of the DLP printing technology is the same as in the rest of SL technologies. A photopolymer resin becomes solid under effect of UV light radiation. Since DLP printing is a representative of MPSL technology, a whole layer of build model solidifies at the same time. The source of the light in the printer is UV LED that produces light radiation with peak wavelength between 385 – 405 nm. The light is then reflected from the array of micromirrors (DMD), each of them can be tilt into two basic positions ON or OFF. Consequently, the light from UV LED can be either reflected though output optic to the

vat with the built material or absorbed by radiator. Each single mirror reflects one pixel of output image. If the light was reflected, it means that on the screen a "white" pixel will appear, in opposite case we will get a "black" pixel. The screen in DLP printers is a bottom surface of the tank with photopolymer. Therefore, the white pixel means that photopolymer solidifies, and the black pixel means that resin remains liquid. The DMD array in tested printer consists of 1039680 mirrors. Resolution of the projector is WXGA 1280 x 800 px.

During printing of the very first layer, platform goes down till contact with the bottom of the vat. A very small amount of ceramic photopolymer stays between platform and bottom surface of the vat. Due to higher density of ceramic photopolymer, platforms with special surfaces were used. It was necessary for reducing suction force during movement up and for reducing force in opposite direction during movement down. Three types of platform surfaces shown on Fig. 2 were used for force reduction.

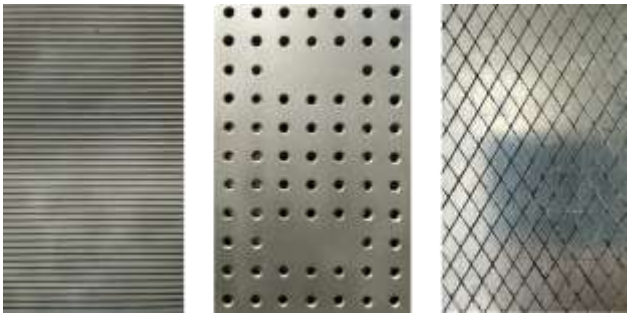

**Figure 2.** Platform surfaces

On the left image of Fig. 2 platform surface with grooves 1 mm width and 0.5 mm deep is presented. On the middle image platform with 2.5 mm diameter wide holes through whole surface is shown. Right picture on Fig. 2 represents platform scratched by laser with grooves approximately 0.5 mm width in diamond orientation. All three platforms have been used for printing from ceramic materials and showed different advantages for different photopolymers and different bottom surfaces of the vat.

The vat for photopolymers has a few options of its bottom surface. It can be borosilicate glass without any coating or with thin layer of polydimethylsiloxane (PDMS) for reduction of suction forces. Also, it is possible to use the vat with fluorinated ethylene propylene (FEP) film tighten on the bottom side without any support.

The printer is also able to measure force that appears during unsticking of a model from the vat. It makes feedback-based control of printing process possible.

Main parameters of the DLP printer are shown in the Tab 1.

| Parameter | Value |
|---|---|
| XY resolution | 65 µm |
| Z axis resolution | 5 µm |
| Suggested layer thickness | 25 – 100 µm |
| Suggested speed | 10 – 25 mm/h |
| Light wavelength | 385 – 405 nm |
| Build volume | 97 x 60 x 100 mm |
| Load cell capacity | up to 500 N |

***Table 1.*** *The printer specification*

### *2.2 Ceramic printing setup*

The process of ceramic printing by DLP technology is shown on Fig. 3.

The first step is to prepare a 3D model for ceramic printing and shrinkage of the final part should be respected during designing. The easiest way is to gain the whole part by coefficient of shrinkage. For getting more precise results, different structures inside designed object should be gained by their own coefficient of shrinkage. For example, the wall with thickness of 2 mm will have a different shrinkage then the column 2 mm wide.

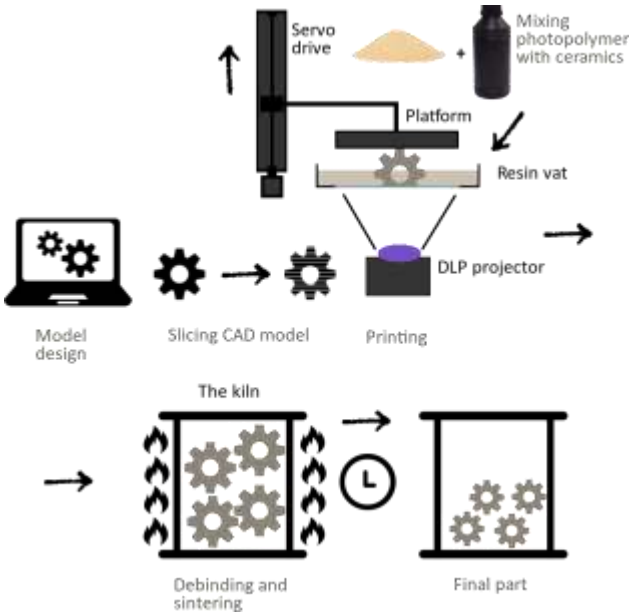


**Figure 3**. Scheme of ceramic printing process

The next step is slicing of a 3D model. There is no big difference between slicing for ceramic and photopolymer printing, therefore it can be provided by general software for DLP printer.

Printing process is very dependent on viscosity of build material. Photopolymer with ceramic parts should be mixed well before pouring into the vat due to different mass of ceramic and photopolymer particles. Printing of ceramic polymers does not have many differences with printing process of general photopolymers. But due to higher viscosity of the ceramic polymers proper filling of the next layer of the model should be ensured. For this task the best results were achieved with platform with holes inside, which stored build material during movements between layers. The worse results we have gotten with scratched platform. For each platform shown on Fig. 2, consumption of photopolymer resin was higher than for smooth platform.

For ceramic printing, lighting strategy is more important than for general photopolymer printing. We have given a different amount of light energy for the first layer, for the layers with supports and for the main part of the model.

When printing is finished, and the green body is built the model should be washed well for preventing undesirable solidification. For the general photopolymer printing post-curing process is necessary for getting crosslink structures. In the case of ceramic printing, this process is not necessary because of consequent debinding and sintering of green body. These steps are provided in a kiln by controlled thermal process. During debinding process, binder polymer releases from a model.

Then, by sintering, solid mass is forming from the ceramic filler. During these processes, green body shrinks and becomes a final part.

The final part always has smaller dimensions than green body due to removing a binder during debinding process. Reduced mass depends on the type of build material, especially on proportion of ceramic filler in it [Halloran 2011].

Thermal treatment curve for postprocess drying, debinding and sintering of a green body in a kiln is shown on Fig.4. Process starts from drying, where temperature is increasing by the ramp 24 °C/h till 150 °C. Then debinding process starts. It is the most crucial process, in which temperature is increasing by slower ramp 12 °C/h till 600 °C. The next step is sintering with much faster ramp 108 °C/h till maximum temperature 1060 °C. Then free cooling follows. Whole process takes above 60 hours. And for each build material optimal ramps should be found.

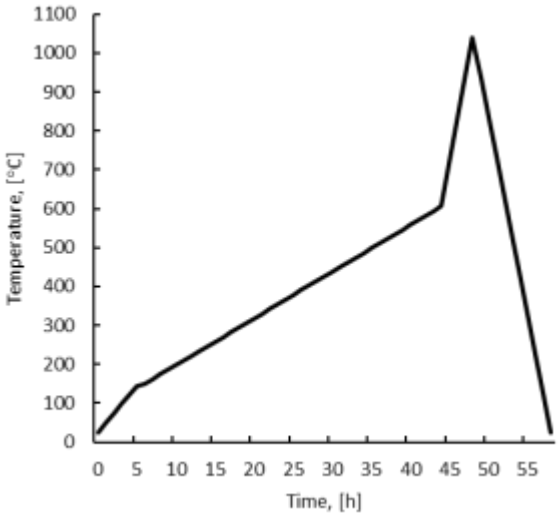


**Figure 4.** Thermal treatment curve

### 2.3 *Building material*

We used a Vitrolite photopolymer resin by Tethon 3D as a build material. It is a mixed glassed ceramic resin, which has high strength and low porosity after firing in the kiln with relatively low temperature. Manufacturer claims shrinkage approximately 17%, depending on the geometry of printed object. Key physical characteristics of the filler are presented below:

- Mean particle size of 7.5 µm
- White to off-white color
- Glass content >87-95%
- Index of refraction is 1.495
- Inflammable, non-toxic
- Low oil absorption

### 2.4 *Printing process*

For shrinkage study we chose to design hollow instead of solid models. This choice was made for making experiment less dependent on the model dimensions, especially on wall thickness. From previous experiments we found that the thicker a wall of the model, the more complicated debinding process is, because results are influenced by amount of polymer that should be released from the green body. Designed hollow cube with supports is shown on Fig. 5.

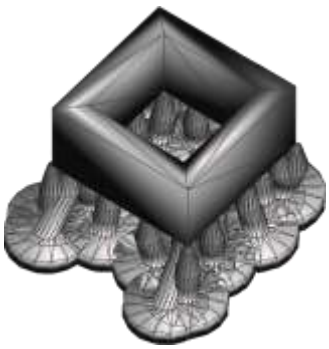

**Figure 5.** Hollow square model

Hollow squares have dimensions 10 x 10 x 5 mm. Supports increased height to 10 mm approximately. Wall thickness of each side of the model is 1.5 mm. In total 9 batches of hollow square models has been printed, each batch contains 6 individual hollow squares. The models were sliced for 50 µm, 75 µm and 100 µm layer thicknesses and each were cured for 3, 5, and 7 seconds, respectively. Printing parameters of each batch are shown in the Table 2.

| Batch No | Layer thickness, µm | Curing time, s | | |
|---|---|---|---|---|
| | | First layer | Support layers | Main layers |
| 1 | 100 | 13 | 9 (layers 2-50) | 7 (layers 51-100) |
| 2 | 100 | 13 | 7 | 5 |
| 3 | 100 | 13 | 5 | 3 |
| 4 | 75 | 13 | 9 (layers 2-67) | 7 (layers 68-134) |
| 5 | 75 | 13 | 7 | 5 |
| 6 | 75 | 13 | 5 | 3 |
| 7 | 50 | 13 | 9 (layers 2-100) | 7 (layers101-200) |
| 8 | 50 | 13 | 7 | 5 |
| 9 | 50 | 13 | 5 | 3 |

***Table 2.*** *Lighting strategy of hollow square printing*

Printed batch before washing is shown on Fig. 6. After printing all batches were washed in isopropyl and measured. Then thermal treatment process was provided according to curve shown on the Fig. 4. Total firing took above 48 hours and with free cooling whole process took approximately 60 hours. After thermal treatment samples were measured again. Green bodies were fired with supports because in previous experiments it was found that samples without supports are more susceptible to bending during debinding.

**Figure 6.** Printed batch before washing

## 3 RESULTS

Printing from a ceramic photopolymer is more sensitive to overgrowth then classical photopolymer printing. Overgrowth is defined as difference between originally exposed and actual length [Mitteramskogler 2014]. This effect can be observed on Fig. 7 that shows green bodies from different batches.

**Figure 7.** Green bodies after washing

On Fig. 7 samples from the first, the second and the third batches are shown (from left to right). The geometrical overgrowth reduces as curing time decreases. Batch 1 has thicker walls with uneven surface and batch 3 has thinner walls with better surface finish. This effect arises due to light scattering of glass particles in resin and should be included in pre-processing adjustments of 3D model. In Tab. 3 mean values of wall thickness overgrowth for both directions and all samples from the batch are shown.

| Batch No | Cure time, s | Layer thickness, µm | Mean overgrowth, % |
|---|---|---|---|
| 1 | 7 | 100 | 3.29 |
| 2 | 5 | 100 | 2.76 |
| 3 | 3 | 100 | 1.51 |
| 4 | 7 | 75 | 3.76 |
| 5 | 5 | 75 | 3.25 |
| 6 | 3 | 75 | 1.69 |
| 7 | 7 | 50 | 6.1 |
| 8 | 5 | 50 | 3.85 |
| 9 | 3 | 50 | 3.17 |

***Table 3.*** *Wall thickness overgrowth of green bodies*

As we can observe, overgrowth is higher with longer cure time and smaller layer thickness. Value of actual overgrowth should be included for each individual printing setup during model design before printing. On Fig. 8 the diagram of wall overgrowth in green bodies is shown.

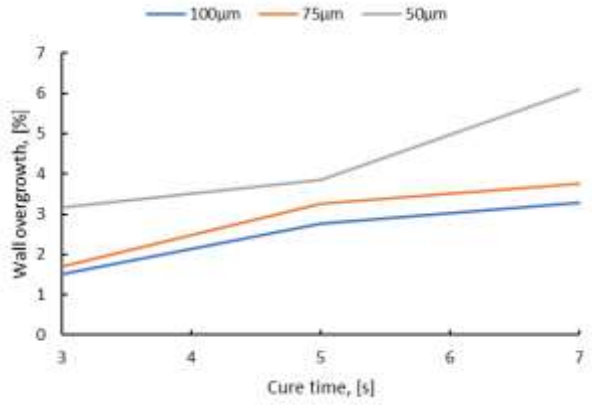


**Figure 8.** Representation of wall overgrowth

After finishing of thermal treatment process each final model was released from supports, checked for cracks and other damages. Also, each sample in each batch was measured and its shrinkage was calculated according to following formula:

$$Shrinkage(\%) = \frac{dimention\ before\ firing - dimention\ after\ firing}{dimention\ before\ firing} \cdot 100$$

Dimensions of hollow squares were measured at 3 points (2 corners and middle) of both outside and inside squares and its average was taken. 3 pairs of groups with same layer thickness and different cure time are analyzed at once for their overall dimensional shrinkage (outside, inside and thickness shrinkages on X and Y axis).

Values of mean shrinkage for each batch are shown in the Tab. 4. As we can observe, shrinkage for each batch is not significantly dependent on printed parameters as oppose to wall overgrowth. For each batch shrinkage is approximately equal to 20 %. For samples inside batches variances are a bit higher but no dependences between them were found. Box plot for them is shown on Fig. 9.

| Batch No | Cure time, s | Layer thickness, µm | Mean shrinkage, % |
|---|---|---|---|
| 1 | 7 | 100 | 20 |
| 2 | 5 | 100 | 19.26 |
| 3 | 3 | 100 | 19.74 |
| 4 | 7 | 75 | 19.76 |
| 5 | 5 | 75 | 19.55 |
| 6 | 3 | 75 | 20.06 |
| 7 | 7 | 50 | 19.1 |
| 8 | 5 | 50 | 19.6 |
| 9 | 3 | 50 | 19.95 |

***Table 4.*** *Shrinkage of final parts after firing*

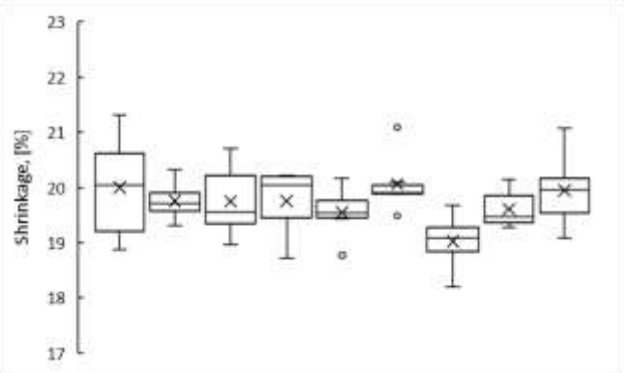


**Figure 9.** Shrinkage of samples in each batch. From left to right batches from 1 to 9

## 4 CONCLUSIONS

Experiments and methods described in this article show ways in improving the quality of ceramic 3D parts printed using DLP technology. Shrinkage value should be measured for each ceramic build material since it depends on the amount of binder inside ceramic photopolymer and does not depend on layer thickness and curing time. As we can see from experiments, obtained value of shrinkage for tested material slightly differs from the value claimed by supplier. It can be caused by different printing parameters or by influence of other factors. That is why, before using ceramic materials in DLP 3D printers it is important to calculate shrinkage for each build material that is going to be used and to find an appropriate thermal treatment curve for a printed model. It can significantly increase a quality of final part.

**ACKNOWLEDGMENTS**

The research reported in this paper was supported by targeted support for specific university research within the student grant competition TUL (Project 21224 – Stereolithography-based 3D printing of ceramic and composite materials).

**REFERENCES**

[Agarwala 1995] Agarwala, M. K. *et al.* Structural Ceramics by Fused Deposition of Ceramics, *Solid Freeform Fabrication Symposium*, 1995, pp. 1–8.

[Agarwala 1996] Agarwala, M. K. *et al.* Fused deposition of ceramics and metals: an overview, *Proceedings of Solid Freeform Fabrication Symposium*, 1996, pp. 385–392.

[Dudley 2003] Dudley, D., Duncan, W. M. and Slaughter, J. Emerging digital micromirror device (DMD) applications, in *SPIE Proceedings*, 2003, p. 14. doi: 10.1117/12.480761.

[Felzmann 2012] Felzmann, R. *et al.* Lithography-based additive manufacturing of cellular ceramic structures, in *Advanced Engineering Materials*, 2012, pp. 1052–1058. doi: 10.1002/adem.201200010.

[Franks 2017] Franks, G. V. *et al.* Colloidal processing: enabling complex shaped ceramics with unique multiscale structures, *Journal of the American Ceramic Society*, 2017, 100(2), pp. 458–490. doi: 10.1111/jace.14705.

[Gmeiner 2015] Gmeiner, R. *et al.* Stereolithographic ceramic manufacturing of high strength bioactive glass, *International Journal of Applied Ceramic Technology*, 2015, 12(1), pp. 38–45. doi: 10.1111/ijac.12325.

[Griffith 2005] Griffith, M. L. and Halloran, J. W. Freeform Fabrication of Ceramics via Stereolithography, *Journal of the American Ceramic Society*, 2005, 79(10), pp. 2601–2608. doi: 10.1111/j.1151-2916.1996.tb09022.x.

[Halloran 2011] Halloran, J. W. *et al.* Photopolymerization of powder suspensions for shaping ceramics, *Journal of the European Ceramic Society*, 2011, 31(14), pp. 2613–2619. doi: 10.1016/j.jeurceramsoc.2010.12.003.

[Hull 1986] Hull, C. W. Apparatus for production of three-dimensional objects by stereolithography, 1986, *US Patent 4,575,330*. doi: 10.1145/634067.634234.

[Li 2017] Li, K. and Zhao, Z. The effect of the surfactants on the formulation of UV-curable SLA alumina suspension, *Ceramics International*, 2017, 43(6), pp. 4761–4767. doi: 10.1016/j.ceramint.2016.11.143.

[Lian 2017] Lian, Q. *et al.* Oxygen-controlled bottom-up mask-projection stereolithography for ceramic 3D printing, *Ceramics International*, 2017, 43(17), pp. 14956–14961. doi: 10.1016/j.ceramint.2017.08.014.

[Mitteramskogler 2014] Mitteramskogler, G. *et al.* Light curing strategies for lithography-based additive manufacturing of customized ceramics, *Additive Manufacturing*, 2014, 1, pp. 110–118. doi: 10.1016/j.addma.2014.08.003.

[Shwentenwein 2015] Schwentenwein, M. and Homa, J. Additive manufacturing of dense alumina ceramics, *International Journal of Applied Ceramic Technology*, 2015, 12(1), pp. 1–7. doi: 10.1111/ijac.12319.

[Travitzky 2014] Travitzky, N. *et al.* Additive manufacturing of ceramic-based materials, *Advanced Engineering Materials*, 2014, 16(6), pp. 729–754. doi: 10.1002/adem.201400097.

[Vail 1992] Vail, N. K. and Barlow, J. W. Ceramic Structures by Selective Laser Sintering of Microencapsulated, Finely Divided Ceramic Materials, in Marcus, H.L., Beaman, J.J., Barlow, J.W., Bourell, D.L., Crawford, R. H. (ed.) *Proceedings of the Solid Freeform Fabrication Symposium*. Austin: The University of Texas at Austin, 1992, pp. 124–130.

[Wohlers 2016] Wohlers, T. *Wohlers Report 2016. 3D Printing and Additive Manufacturing State of the Industry*, *Wohlers Report 2016,* 2016. doi: ISBN 978-0-9913332-2-6.

[Wong 2012] Wong, K. V. and Hernandez, A. A Review of Additive Manufacturing, *ISRN Mechanical Engineering*, 2012, pp. 1–10. doi: 10.5402/2012/208760.

[Yoo 1993] Yoo, J. *et al.* Structural ceramic components by 3D printing, *Solid Freeform Fabrication Symposium*, 1993, pp. 40–50.

**CONTACTS:**

Ing. Iaroslav Kovalenko
Technical University of Liberec, Faculty of Mechanical Engineering, Department of Manufacturing Systems and Automation
Studentska 1402/2, Liberec, 46117, Czech Republic
+420 485353282, iaroslav.kovalenko@tul.cz